Contribution from the Department of Chemistry,
The University of North Carolina at Charlotte, Charlotte, North Carolina 28223

Complexes of Ruthenium(II) with $bpmRe(CO)_3Cl$ and $HAT(Re(CO)_3Cl)_2$ as Ligands: Syntheses and Redox and Luminescence Properties

Ram Sahai, D. Paul Rillema,* Randy Shaver, Shawn Van Wallendael, Donald C. Jackman, and Massoud Boldaji

Received August 17, 1988

A series of mixed-metal complexes containing ruthenium and rhenium are reported. The new complexes are $[(bpy)Ru(bpmRe(CO)_3Cl)_2](PF_6)_2$, $[(bpy)_2RuHAT(Re(CO)_3Cl)_2](PF_6)_2$, and $[Ru(bpmRe(CO)_3Cl)_3](PF_6)_2$. Optical transitions in the visible–UV spectrum are dominated by the presence of the ruthenium heterocycles that have absorption coefficients for the low-energy transition 1 order of magnitude greater than that of the rhenium chromophore. The low-energy transition blue-shifts in the series $[(bpy)_2Ru(bpmRe(CO)_3Cl)]^{2+}$ (558 nm) < $[(bpy)Ru(bpmRe(CO)_3Cl)_2]^{2+}$ (531 nm) < $[Ru(bpmRe(CO)_3Cl)_3]^{2+}$ (501 nm). Polarographic half-wave potentials of the metal-centered oxidations and the bridging-ligand reductions shift positively as the number of $Re(CO)_3Cl$ units increase. The $E_{1/2}$ values for the $[(bpy)_nRu(bpmRe(CO)_3Cl)_{3-n}]^{2+/+}$ couple in the series with n = 0–2 were −0.21, −0.33, and −0.41 V vs SSCE, respectively. Two complexes, $[(bpy)Ru(bpmRe(CO)_3Cl)_2]^{2+}$ and $[Ru(bpmRe(CO)_3Cl)_3]^{2+}$, were found to luminesce weakly at room temperature in acetonitrile with lifetimes of 942 and 847 ns, respectively. In many respects, the mixed-metal complexes are shown to behave as if the $bpmRe(CO)_3Cl$ and $HAT(Re(CO)_3Cl)_2$ chromophores are ligands coordinated to ruthenium(II).

Introduction

Recently, our research contributions have demonstrated the ability to design metallic clusters by the assembly of simple molecular components in a rational way.[1,2] We have, for example, reported the synthesis of $[Ru(bpqRu(bpy)_2)_3]^{8+}$ and $[Ru(bpqPtCl_2)_3]^{2+}$, where bpq is 2,3-bis(2-pyridyl)quinoxaline and bpy is 2,2′-bipyridine.[2] The rational design takes advantage of bidentate chelating sites on both sides of heterocyclic ligands (see Figure 1) for effecting bridging from one metal center to the other. The foundation of the oligomer is a ruthenium core complex, e.g. $Ru(bpq)_3^{2+}$, followed by attachment of the other desired metal complex or complexes. In this paper we have extended our work to include multimetallic ruthenium(II)/rhenium(I) complexes based on the bridging ligands 2,2′-bipyrimidine and benzo[1,2-*b*:3,4-*b*′:5,6-*b*″]tripyrazine (HAT).

Vogler and Kisslinger[3] gave a brief report on the synthesis and properties of the mononuclear complex $(bpm)Re(CO)_3Cl$ and binuclear complexes $(Re(CO)_3Cl)_2bpm$ and $[(bpy)_2RubpmRe(CO)_3Cl]$. The chemistry followed in part from the related 2,2′-bipyridine analogue $(bpy)Re(CO)_3Cl$, which is reported to have an emissive electron-transfer excited state.[4-6] In related excited-state donor/acceptor work, we have recently reported the synthesis and properties of $[(bpm)Re(CO)_3L]^{n+}$, where L is *N*-methyl-4,4′-bipyridinium ion (n = 2) and 10-(4-picolyl)-phenothiazine (n = 1).[7]

The new complexes reported here are $[(bpy)Ru(bpmRe(CO)_3Cl)_2]^{2+}$, $[Ru(bpmRe(CO)_3Cl)_3]^{2+}$, and $[(bpy)_2RuHAT(Re(CO)_3Cl)_2]^{2+}$. The complexes were prepared as part of our efforts to design multielectron-transfer catalysts. The preparations and redox, spectral, and luminescence properties of these complexes will be described in this paper along with more details on the properties of their precursors.

Experimental Section

Materials. $RuCl_3 \cdot 3H_2O$ was donated by Johnson-Mathey, Inc. $Re(CO)_5Cl$, 2,2′-bipyridine, and 2,2′-bipyrimidine were purchased commercially. Solvents used for preparations and spectroscopic studies were of HPLC grade. Solvents used for electrochemical studies were dried over 4-Å molecular sieves for 48 h before use. Electrolytes, tetraethylammonium perchlorate (TEAP) and tetrabutylammonium hexafluorophosphate (TBAH), were of electrograde from Southwestern Analytical. TATB (1,3,5-triamino-2,4,6-trinitrobenzene) was obtained from Chemtronics, Sannanoa, NC. Elemental analyses were performed by Atlantic Microlab, Inc., and accompany the paper as supplemental information.

Preparation of Compounds. $[Ru(bpy)_2(bpm)](ClO_4)_2$,[8] $[Ru(bpy)(bpm)_2](PF_6)_2$,[8] $[Ru(bpm)_3](ClO_4)_2$,[8] and $[Ru(bpy)_2(HAT)](PF_6)_2$[9] were prepared by literature methods.

$[Ru(bpy)_2(bpmRe(CO)_3Cl)](ClO_4)_2$. The procedure to prepare this complex was an adaptation of the one reported by Vogler and Kisslinger.[3] Approximately 0.30 mmol of $[Ru(bpy)_2(bpm)](ClO_4)_2$ was dissolved in 100 mL of CH_3OH. In a separate container, 0.35 mmol of $Re(CO)_5Cl$ was dissolved in 50 mL of CH_3OH by sonication. The two solutions were added together and refluxed for 8 h under a nitrogen blanket. The resulting solution was allowed to cool, and the volume was reduced to 50 mL with a rotary evaporator. A saturated methanol solution of sodium perchlorate was added dropwise to crystallize the product. The precipitate was collected by suction filtration, washed with ethyl ether, and dried under vacuum. Yield: 0.31 g (95%). *Caution!* Perchlorate salts are potentially explosive.

$[Ru(bpy)(bpmRe(CO)_3Cl)_2](PF_6)_2$. Approximately 0.18 mmol of $[Ru(bpy)(bpm)_2](PF_6)_2$ was suspended in 150 mL of CH_3OH. A 0.40-mmol quantity of $Re(CO)_5Cl$ was dissolved in 50 mL of CH_3OH by sonication. The $Re(CO)_5Cl$ solution was added to the suspension, and the resulting mixture was reluxed under a N_2 blanket for 6 h. The resulting deep red solution was filtered and reduced in volume to 50 mL. Deep red microcrystalline material precipitated upon standing overnight. The product was isolated by filtration, washed with ether, and air-dried. Yield: 0.24 g (90%).

$[Ru(bpmRe(CO)_3Cl)_3](ClO_4)_2$. Approximately 0.30 mmol of $[Ru(bpm)_3]Cl_2$ was dissolved in 50 mL of CH_3OH. One millimole of $Re(CO)_5Cl$ was dissolved in 200 mL of CH_3OH by sonication. The two solutions were added together and refluxed for 9 h under a N_2 blanket. The resulting solution was allowed to cool, and the volume was reduced to 75 mL with a rotary evaporator. A saturated methanol solution of sodium perchlorate was added dropwise to crystallize the product. The precipitate was collected by suction filtration, washed with CH_3OH, and dried under vacuum. Yield: 0.44 g (87%). *Caution!* Perchlorate salts are potentially explosive.

Benzo[1,2-*b*:3,4-*b*′:5,6-*b*″]tripyrazine (HAT). HAT was prepared by a modification of Roger's procedure.[10] A magnetic stirring bar was added to a 1-L, three-necked round-bottom flask, which was then fitted with a ground-glass stopper, a Dewar condenser with a nitrogen line, and a gas-inlet tube. Approximately 400 mL of ammonia was condensed into the flask after it was immersed in a dry ice/2-propanol bath and the Dewar was filled with a dry ice/2-propanol mixture. A 137-mL quantity of methanol was then added, followed by slow addition of 7.2 g of TATB (1,3,5-triamino-2,4,6-trinitrobenzene). The flask was then allowed to

(1) Sahai, R.; Rillema, D. P. *Inorg. Chim. Acta* **1986**, *188*, L35.
(2) Sahai, R.; Rillema, D. P. *J. Chem. Soc., Chem. Commun.* **1986**, 1133.
(3) Vogler, A.; Kisslinger, J. *Inorg. Chim. Acta* **1986**, *115*, 193.
(4) Geoffroy, G. L.; Wrighton, M. S. *Organometallic Photochemistry*; Academic Press: New York, 1979; and references therein.
(5) (a) Wrighton, M. S.; Morse, D. L. *J. Am. Chem. Soc.* **1974**, *96*, 998. (b) Giordano, P. J.; Wrighton, M. S. *J. Am. Chem. Soc.* **1979**, *101*, 2888.
(6) (a) Caspar, J. V.; Meyer, T. J. *J. Phys. Chem.* **1983**, *87*, 952. (b) Caspar, J. V.; Sullivan, B. P.; Meyer, T. J. *Inorg. Chem.* **1984**, *23*, 2104.
(7) Winslow, L. N.; Rillema, D. P.; Welch, J. H.; Singh, P. *Inorg. Chem.*, in press.
(8) Rillema, D. P.; Allen, G.; Meyer, T. J.; Conrad, D. *Inorg. Chem.* **1983**, *22*, 1617.
(9) Masschelein, A.; Kirsch-De Mesmaeker, A.; Verhoven, C.; Nasielski-Henkens, R. *Inorg. Chim. Acta* **1987**, *129*, L13.
(10) Rogers, D. Z. *J. Org. Chem.* **1986**, *51*, 3904.
(11) Rillema, D. P.; Mack, K. *Inorg. Chem.* **1982**, *21*, 3849.

0020-1669/89/1328-1022$01.50/0

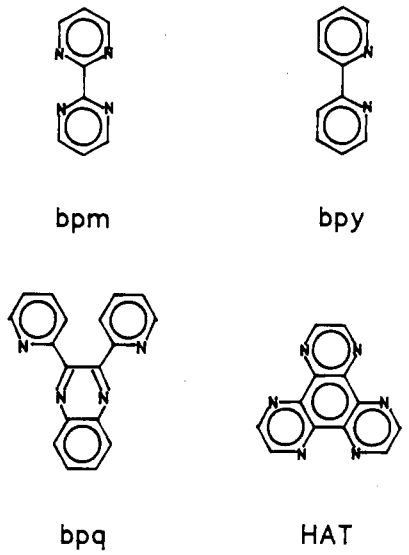

Figure 1. The ligands.

Table I. Carbonyl Stretching Frequencies for Ruthenium(II)/Rhenium(I) Complexes[a]

compd	freq, cm^{-1}
$Re(CO)_5Cl$	2151, 2044, 2013, 1979
$(bpm)Re(CO)_3Cl$	2033, 1906 (sh), 1899
$[(Re(CO)_3Cl)_2bpm]$	2028, 1908
$[(bpy)_2Ru(bpmRe(CO)_3Cl)](ClO_4)_2$	2034, 1928 (sh), 1915
$[(bpy)Ru(bpmRe(CO)_3Cl)_2](PF_6)_2$	2034, 1934 (sh), 1906
$[Ru(bpmRe(CO)_3Cl)_3](ClO_4)_2$	2036, 1913
$[(bpy)_2RuHAT(Re(CO)_3Cl)_2](PF_6)_2$	2026, 1919

[a] KBr pellets; frequency error ±2 cm^{-1}.

warm to −33 °C. Then sodium was freshly cut into small pieces under toluene, and 16.2 g was added to the flask over a period of 6 h. The Dewar condenser was removed, and ammonia was vented away under a stream of nitrogen. The cream-colored solid that remained was suction-filtered on a fine frit and washed with four 30-mL portions of absolute ethanol followed by three 30-mL ethyl ether washings. The solid was allowed to dry briefly at room temperature and was then added to 50 mL of stirred, ice-chilled 40% glyoxal over a period of approximately 10 min. The suspension was removed from the ice bath and allowed to stir at room temperature for 1 h. It was then poured into 300 mL of H_2O and stirred for 12 h.

The resulting precipitate was collected by suction filtration, washed first with water and then with ethanol until the washings were clear, and then washed with ethyl ether. The light brown powder (4.7 g of crude HAT) was collected and dried. It was placed in a Soxhlet extractor and extracted with chloroform for 71 h. A yellow powder was obtained after removal of chloroform. It was purified by the chromatographic techniques described by Rogers.[10] Yield: 2.3 g (62%).

$[Ru(bpy)_2HAT(Re(CO)_3Cl)_2](PF_6)_2$. A solution of 80 mg (0.22 mmol) of $Re(CO)_5Cl$ in 100 mL of methanol was added to 100 mg (0.106 mmol) of $[Ru(bpy)_2HAT](PF_6)_2$ in 300 mL of methanol. The resulting solution was refluxed for 72 h and then cooled to room temperature. The reaction solution was concentrated to approximately 40 mL and chilled overnight at −5 °C. The solids that formed were removed by suction filtration, and the filtrate was then added to cold anhydrous ether, producing a purple precipitate. The precipitate was collected by suction filtration and dried under vacuum. Yield: 80 mg (49%).

$[(bpm)Re(CO)_3Cl]$. A 100-mg quantity of $Re(CO)_5Cl$ was dissolved in 75 mL of methanol by sonication. Then 100 mg of 2,2′-bipyrimidine was added, and the resulting solution was refluxed under N_2 for 3 h. The deep yellow solution was allowed to cool overnight at 4 °C. The yellow material that crystallized was filtered and vacuum-dried. Yield: 115 mg (87%).

$[(Cl(CO)_3Re)_2](bpm)$. Sonication was used to dissolve 205 mg of $Re(CO)_5Cl$ in 150 mL of methanol. This was followed by addition of 48 mg of 2,2′-bipyrimidine. The resulting solution changed color from yellow to red, and finally a deep red crystalline material formed after the solution was refluxed under N_2 for 3 h. The solution was allowed to cool. It was then filtered to remove the precipitate, which was washed with small portions of methanol, then washed with ether, and finally dried under vacuum. Yield: 140 mg (85%).

Physical Measurements. Visible–UV spectra were recorded with a Perkin-Elmer Lambda Array 3840 spectrophotometer. Luminescence spectra were recorded with Perkin-Elmer 650-40 and Spex Fluorolog spectrofluorometers. Cyclic voltammograms were obtained in acetonitrile solutions containing 0.10 M TEAP or 0.10 M TBAH as supporting electrolyte. The measurements were made vs the saturated sodium chloride calomel electrode (SSCE). Electrochemistry was carried out with a PAR 174A polarographic analyzer or a PAR 173 potentiostat in conjunction with a PAR 175 programmer. Cyclic voltammograms were recorded with a YEW Model 3022 X–Y recorder. Luminescence lifetimes were determined with the Molectron nitrogen dye-pumped laser system previously described.[8] Infrared spectra were recorded with a Mattson FTIR spectrometer.

Results

Isomers. $Re(CO)_5Cl$ reacted smoothly with the remote nitrogen sites of coordinated bipyrimidine and HAT to give the desired mixed-metal ruthenium(II)/rhenium(I) complexes. The CO stretching frequencies given in Table I are similar in energy for all the rhenium heterocyclic ligand complexes, including $Re(bpm)(CO)_3Cl$, which can be regarded as a model compound for comparison to the multimetallic complexes. The pattern of two observed CO stretching frequencies in the 2030- and 1900-cm^{-1} regions was also observed for the $Re(bpy)(CO)_3Cl$ analogue.[5] On the other hand, $Re(CO)_5Cl$ exhibited two sets of two vibrational modes located at 2151 and 2013 cm^{-1} and at 2044 and 1979 cm^{-1}. For $Re(CO)_5Cl$ there are clearly different geometric types of CO ligands giving rise to the two sets of CO stretching frequencies whereas, in $(BL)Re(CO)_3Cl$, where BL is either bpm or HAT, only one type of CO ligand is present. This is consistent with the facial isomers for the rhenium tricarbonyl moieties. The observed shoulder on the 1900-cm^{-1} band for some of the complexes in Table I may arise due to different ligands trans to the three CO ligands.

For multimetallic complexes containing more than one $(BL)Re(CO)_3Cl$ unit, there are additional isomers possible. In $(Re(CO)_3Cl)_2bpm$, for example, the chloride ligands can both lie on one side or on opposite sides of the plane defined by the bpm ligand. The physical properties studied for these compounds will not allow us to distinguish among these forms.

Visible–UV Spectra. A summary of the visible–UV spectral properties of the multimetallic complexes are given in Table II and compared to those of their monometallic precursors. The observed transitions are related to metal-to-ligand charge-transfer (MLCT) and intraligand $\pi \rightarrow \pi^*$ transitions. Assignment of the

Table II. Visible–UV Spectra of Ruthenium(II)/Rhenium(I) Complexes in Acetonitrile[a–c]

complex	$d\pi(M) \rightarrow \pi^*(BL)$	$d\pi \rightarrow \pi^*$	$\pi \rightarrow \pi^*$
$[bpmRe(CO)_3Cl]$	384 (2.7×10^3)	310 (sh)	232 (2.3×10^4)
$[(Re(CO)_3Cl)_2bpm]$[d]	480 (3.7×10^3)	350 (6.6×10^3)	
$[(bpy)_2Ru(bpm)]^{2+}$[e]	480 (sh)	422 (9.1×10^3)	284 (5.6×10^4), 236 (4.0×10^4)
$[((bpy)_2Ru)_2bpm]^{4+}$[f]	594 (8.2×10^3)	545 (sh), 411 (2.4×10^4)	280 (7.5×10^4), 243 (sh)
$[(bpy)_2Ru(bpmRe(CO)_3Cl)]^{2+}$	558 (4.5×10^3)	414 (1.6×10^4), 377 (sh)	284 (4.4×10^4), 243 (3.5×10^4)
$[(bpy)Ru(bpmRe(CO)_3Cl)_2]^{2+}$	531 (6.8×10^3)	382 (1.7×10^4), 321 (sh)	285 (sh), 244 (4.3×10^4)
$[Ru(bpmRe(CO)_3Cl)_3]^{2+}$	501 (1.1×10^4)	347 (1.9×10^4)	285 (sh), 240 (5.1×10^4)
$[Ru(bpy)_2HAT]^{2+}$[g]	484 (sh)	432 (1.0×10^4)	277 (5.9×10^4), 207 (4.5×10^4)
$[(Ru(bpy)_2)_2HAT]^{4+}$[g]	572 (1.5×10^4)	490 (1.4×10^4), 405 (1.4×10^4)	276 (1.0×10^5), 243 (sh), 206 (7.4×10^4)
$[(bpy)_2RuHAT(Re(CO)_3Cl)_2]^{2+}$	529 (2.2×10^4)	406 (1.4×10^4)	283 (7.1×10^4), 252 (4.9×10^4)

[a] λ_{max} in nm; error ±1 nm. [b] ϵ values follow in parentheses; units are M^{-1} cm^{-1}; error ±1 M^{-1} cm^{-1}. [c] $T = 25 \pm 2$ °C. [d] In DMF. [e] Reference 8. [f] Reference 11. [g] Reference 9.

Table III. Polarographic Half-Wave Potentials for Various Ruthenium(II)/Rhenium(I) Complexes[a,b]

complex	oxidns $E_{1/2}$, V	redns $E_{1/2}$, V
[bpmRe(CO)$_3$Cl]	1.43 (irr)[c]	−1.03, −1.65 (irr)[c]
[(Re(CO)$_3$Cl)$_2$bpm][d]		−0.30, −1.18 (irr)[c]
[(bpy)$_2$Ru(bpm)]$^{2+}$[e]	1.40	−1.02, −1.45, −1.83[f]
[(bpy)$_2$Ru)$_2$bpm]$^{4+}$[g]	1.69, 1.53	−0.41, −1.08
[(bpy)$_2$Ru(bpmRe(CO)$_3$Cl)]$^{2+}$	1.76, 1.58	−0.41, −1.10, −1.56, −1.81
[(bpy)Ru(bpmRe(CO)$_3$Cl)$_2$]$^{2+}$	1.61[l]	−0.33, −0.48, −1.09, −1.23, −1.80 (irr)[c]
[Ru(bpmRe(CO)$_3$Cl)$_3$]$^{2+}$	1.59[l]	−0.21, −0.35, −0.53[h]
[Ru(bpy)$_2$HAT]$^{2+}$[i]	1.56	−0.84, −1.43, −1.6[f]
[(Ru(bpy)$_2$)$_2$HAT]$^{4+}$[i]	1.78, 1.53[l]	−0.49, −1.06
[(bpy)$_2$RuHAT(Re(CO)$_3$Cl)$_2$]$^{2+}$	1.74 (irr),[c] 1.48	−0.07, −0.44, −0.97, −1.20, −1.45, −1.58[c] (irr), −1.82
HAT[j]		−1.47, −1.62, −1.88[f]
bpm[k]		−1.80

[a] Potentials are in volts vs SSCE; error ±0.02 V; scan rate 200 mV/s. [b] Solutions were 0.10 M in TBAH; the solvent was acetonitrile, unless otherwise noted. [c] Listing is E_p value. [d] Dimethylformamide was the solvent. [e] Reference 8. [f] This work. [g] Reference 11. [h] See Figure 4. [i] Reference 9. [j] Our results are comparable to those of ref 9. [k] Data from: Kawanishi, Y.; Kitamura, N.; Kim, Y.; Tazuka, S. *Riken Q.* **1984**, *78*, 212. [l] Quasi-reversible.

origin of each transition in most of the complexes is difficult due to the presence of different heterocyclic ligands, bpm, HAT, and bpy, and two different metals, ruthenium and rhenium.

To enable an understanding of their visible–UV properties, it is helpful to analyze the spectra in the order of first the simple monometallic precursors, then the homobimetallic complexes, and finally the mixed-metal multimetallic complexes. The low-energy transitions in Table II are assigned as $d\pi(M) \rightarrow \pi^*(BL)$, where M represents either ruthenium(II) or rhenium(I) and BL is either bpm or HAT. For monometallic species, the low-energy transitions fall in the order (bpm)Re(CO)$_3$Cl > [Ru(bpy)$_2$(bpm)]$^{2+}$ > [Ru(bpy)$_2$HAT]$^{2+}$. This means that the lowest energy transition in the series is $d\pi(Ru) \rightarrow \pi^*(HAT)$, then $d\pi(Ru) \rightarrow \pi^*(bpm)$, and finally $d\pi(Re) \rightarrow \pi^*(bpm)$.

A comparison of the low-energy transition of the homobimetallic complexes leads to an understanding of the specific metal associated with the $d\pi(M) \rightarrow \pi^*(BL)$ transitions in mixed-metal complexes. For both rhenium and ruthenium homobimetallic complexes, the low-energy transition is red-shifted approximately 100 nm compared to that of their monometallic parents. The energy ordering of the low-energy transition remains nearly the same as found for their monometallic parents: [(Re(CO)$_3$Cl)$_2$bpm] > [(Ru(bpy)$_2$)$_2$HAT]$^{4+}$ ~ [(Ru(bpy)$_2$)$_2$bpm]$^{4+}$. The $d\pi(Re) \rightarrow \pi^*(bpm)$ transition occurs at higher energy than found for the ^{1}MLCT transition associated with the ruthenium(II) core. Further, the $d\pi(Re) \rightarrow \pi^*(bpm)$ and $d\pi(Ru) \rightarrow \pi^*(bpm)$ transitions occur with a fairly large energy difference of ~100 nm, e.g. 480 nm for [(Re(CO)$_3$Cl)$_2$bpm] and 594 nm for [(Ru(bpy)$_2$)$_2$bpm]$^{4+}$, and with a lower absorption coefficient, e.g. 3.7×10^3 M^{-1} cm^{-1} for [(Re(CO)$_3$Cl)$_2$bpm] compared to 8.2×10^3 M^{-1} cm^{-1} for [(Ru(bpy)$_2$)bpm]$^{4+}$.

The mixed-metal ruthenium(II)/rhenium(I) complexes exhibit a low-energy transition in the 500-nm region that blue-shifts in the sequence [(bpy)$_2$Ru(bpmRe(CO)$_3$Cl)]$^{2+}$ < [(bpy)Ru(bpmRe(CO)$_3$Cl)$_2$]$^{2+}$ < [Ru(bpmRe(CO)$_3$Cl)$_3$]$^{2+}$. This is illustrated in Figure 2. This low-energy absorption is clearly related to $d\pi(Ru) \rightarrow \pi^*(bpm)$ by analogy to the homobimetallic complexes. Compared to that of ruthenium multimetallic complexes, e.g. [Ru(bpmRu(bpy)$_2$)$_3$]$^{8+}$, the ^{1}MLCT spectral region for the ruthenium(II)/rhenium(I) oligomers is simpler due to the presence of only one ruthenium absorbing unit. Their spectral shift, then, is analogous to that found by removal of a bpy ligand and replacing it with bpm in the series [Ru(bpm)$_n$(bpy)$_{3-n}$]$^{2+}$, where $n = 1$–3.[8]

The intermediate energy transitions are labeled $d\pi \rightarrow \pi^*$ without association with a given ligand or metal center. Several are possible including transitions between rhenium and the bridging ligand and transitions between ruthenium and the bipyridine ligands. In addition, two ^{1}MLCT transitions, $d\pi \rightarrow \pi_1^*$, and $d\pi \rightarrow \pi_2^*$, are predicted for each possibility. For Ru(bpy)$_3^{2+}$, the parent in many of these studies, a second ^{1}MLCT transition is predicted approximately 6000 cm^{-1} above the first.[12] Consequently, overlapping absorptions, which are difficult to assign to a given process, are observed.

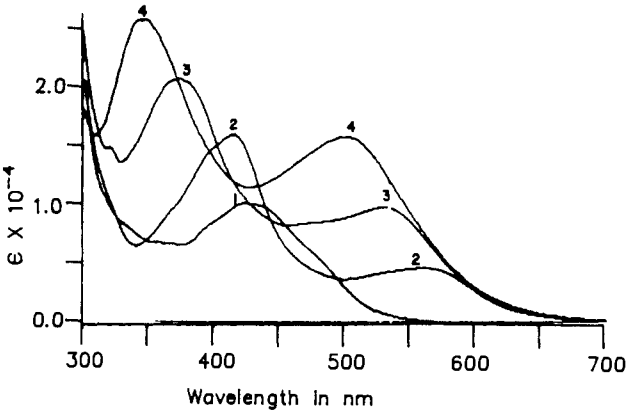

Figure 2. Visible–UV spectra for a series of Ru(II)/Re(I) heterooligomers: (1) [Ru(bpy)$_2$(bpm)]$^{2+}$; (2) [Ru(bpy)$_2$(bpmRe(CO)$_3$Cl)]$^{2+}$; (3) [Ru(bpy)(bpmRe(CO)$_3$Cl)$_2$]$^{2+}$; (4) [Ru(bpmRe(CO)$_3$Cl)$_3$]$^{2+}$.

The high-energy $\pi \rightarrow \pi^*$ transitions also are ambiguous to assign in mixed-ligand systems. The observed spectra in this region are fairly simple. Two absorptions for the multimetallic complexes studied here were generally found near 280 and 240 nm.

Electrochemistry. Redox potentials for the complexes were determined in acetonitrile, except where noted, by cyclic voltammetry and are tabulated in Table III. The redox properties of mixed-metal complexes can be understood by comparison to their monometallic and bimetallic precursors. As illustrated in Figure 3 for (bpm)Re(CO)$_3$Cl, an electrochemically irreversible peak is present at 1.43 V for oxidation of rhenium(I), a reversible wave is present at −1.03 V assigned as a bpm-based reduction, and an irreversible wave is observed at −1.65 V due to reduction of rhenium(I). As also shown in Figure 3, the ruthenium monomer, [(bpy)$_2$Ru(bpm)]$^{2+}$, exhibits a reversible Ru(III)/Ru(II) couple at 1.40 V, a reversible wave centered at −1.02 V assigned as a bpm-based reduction, and a set of two reversible waves located at −1.45 and −1.83 V assigned as bpy-based reductions. [Ru(bpy)$_2$HAT]$^{2+}$ exhibits similar behavior (not shown). A reversible Ru(III)/Ru(II) couple is observed at 1.56 V, a reversible reduction is observed at −0.48 V assigned to the HAT ligand, and two bpy ligand reductions are found at −1.43 and −1.6 V.[9]

The cyclic voltammetric data for [(Re(CO)$_3$Cl)$_2$bpm], [((bpy)$_2$Ru)$_2$bpm]$^{4+}$, and [(Ru(bpy)$_2$)$_2$HAT]$^{4+}$ are also given in Table III. For [(Re(CO)$_3$Cl)$_2$bpm], the rhenium(I) oxidation is shifted outside the solvent window (DMF); the ligand reduction wave and rhenium(I) reductions are shifted positively 0.5–0.7 V relative to the monometallic complex. For [((bpy)$_2$Ru)$_2$bpm]$^{4+}$ and [(Ru(bpy)$_2$)$_2$HAT]$^{4+}$ two reversible one-electron waves (one per Ru(II) center) in the positive region were found at 1.53 and 1.69 V and at 1.53 and 1.78 V, respectively.[8,11] The bridging ligand reductions were shifted 0.4–0.6 V positively compared to their

(12) $\Delta E_p = |E_{p,ox} - E_{p,red}|$.

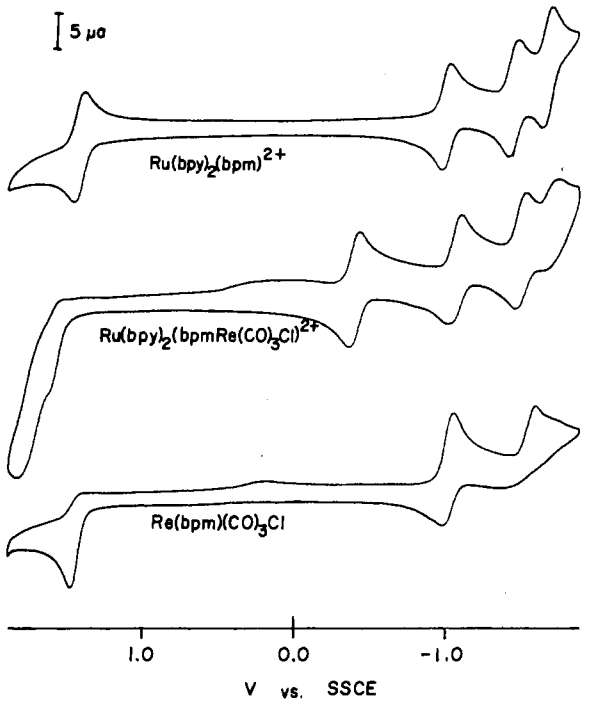

Figure 3. Comparison of cyclic voltammograms for $[Ru(bpy)_2(bpm)]^{2+}$, $[Re(bpm)(CO)_3Cl]$, and $[Ru(bpy)_2(bpmRe(CO)_3Cl)]^{2+}$ in acetonitrile.

monometallic precursors. The first two reductions were assigned to the bridging ligands.[11] In the case of $[(Ru(bpy)_2)_2bpm]^{4+}$, these were the first and second reductions of the bpm ligand as illustrated in eq 1 and 2.

$$[(Ru^{II}(bpy)_2)_2bpm]^{4+} + e^- \rightarrow [(Ru^{II}(bpy)_2)_2bpm^-]^{3+} \quad (1)$$

$$[(Ru^{II}(bpy)_2)_2bpm^-]^{3+} + e^- \rightarrow [(Ru^{II}(bpy)_2)_2bpm^{2-}]^{2+} \quad (2)$$

Cyclic voltammograms for the mixed-metal complexes contained features of both the monometallic and homobimetallic complexes. The cyclic voltammogram for $[Ru(bpy)_2(bpmRe(CO)_3Cl)]^{2+}$ is shown in Figure 3 and compared to the ones for $Re(bpm)(CO)_3Cl$ and $[Ru(bpy)_2(bpm)]^{2+}$. The wave in the positive region near 1.75 V consists of the reversible Ru(III/II) couple and the irreversible rhenium(I) oxidation nearly superimposed. The more positive wave most likely corresponds to the irreversible rhenium(I) oxidation and the shoulder to the Ru(III/II) couple. A similar situation was found for $[Ru(bpy)_2HAT(Re(CO)_3Cl)_2]^{2+}$ upon oxidation, although the Ru(III/II) couple in this case was masked by the rhenium(I) irreversible oxidation wave. Quasi-reversible waves (ΔE_p = 120–140 mV)[12] for the trimetallic and tetrametallic complexes, $[(bpy)Ru(bpmRe(CO)_3Cl)_2]^{2+}$ and $[Ru(bpmRe(CO)_3Cl)_3]^{2+}$, were observed near 1.60 V and probably are overlapping Ru(III/II) and Re(II/I) couples. This is illustrated in Figure 4. An irreversible wave near 0.3 V is observed after scanning through the rhenium(I) oxidation. This is illustrated in both Figures 3 and 4. The wave at ~0.3 V may be due to Cl_2 reduction, where Cl_2 is formed via a secondary process involving ligand oxidation following oxidation of Re(I) to Re(II).

Reductions of the bimetallic complex $[(bpy)_2Ru(bpmRe(CO)_3Cl)]^{2+}$ are shown in Figure 3. The first and second reductions of the bridging ligand are located at −0.41 and −1.10 V. The reductions centered at −1.56 and −1.81 V exhibit greater cathodic peak currents than the bpm-based reductions and hence have i_c/i_a ratios greater than 1. These are likely overlapping bpy and Re(I) reductions, respectively.

A continual series of reduction waves are observed for $[(bpy)_2RuHAT(Re(CO)_3Cl)_2]^{2+}$. At least the first four reductions involve successive reductions of the HAT ligand. The remaining reductions may be HAT or bpy centered with perhaps one exception. An irreversible wave is present at −1.60 V, which most likely is a rhenium-based reduction by analogy to the other

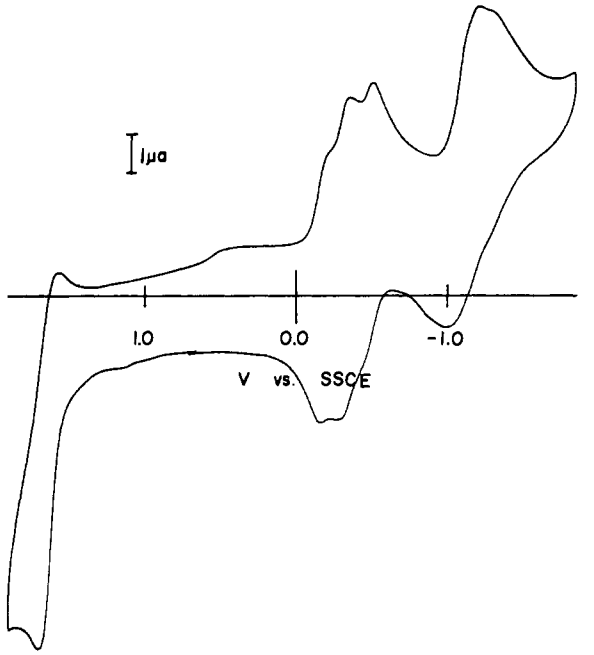

Figure 4. Cyclic voltammogram for $[Ru(bpmRe(CO)_3Cl)_3]^{2+}$ in acetonitrile.

rhenium complexes. For the other waves, i_c/i_a ratios are near 1 and ΔE_p values range from 60–90 mV as expected for a one-electron-transfer process.[13]

For $[Ru(bpmRe(CO)_3Cl)_3]^{2+}$ and $[(bpy)Ru(bpmRe(CO)_3Cl)_2]^{2+}$, a series of bpm ligand reductions were observed as illustrated in Figure 4. The first set of three reductions are resolvable whereas the second set are not. The first three reductions have $E_{1/2}$ values of −0.21, −0.35, and −0.53 V, and their assignments are illustrated in eq 3–5. The second set have E_p

$$Ru^{II}(bpmRe^{I}(CO)_3Cl)_3 + e^- \rightarrow Ru^{II}(bpm^-Re^{I}(CO)_3Cl)(bpmRe^{I}(CO)_3Cl)_2 \quad (3)$$

I II

$$II + e^- \rightarrow Ru^{II}(bpm^-Re^{I}(CO)_3Cl)_2(bpmRe^{I}(CO)_3Cl) \quad (4)$$

III

$$III + e^- \rightarrow Ru^{II}(bpm^-Re^{I}(CO)_3Cl)_3 \quad (5)$$

values of −1.24, −1.29, and −1.35 V for the reduction waves but poorly defined oxidation wave counterparts. The trinuclear $[(bpy)Ru(bpmRe(CO)_3Cl)_2]^{2+}$ complex follows a similar pattern upon reduction. In this case, two sets of two reductions corresponding to the first and second reduction of each bridging ligand were observed. These occur at $E_{1/2}$ values of −0.33 and −0.48 V for the first set and at −1.09 and −1.23 V for the second set. The reduction at −1.80 V is irreversible and most likely corresponds to reduction of rhenium(I).

Luminescence. The luminescence properties of the complexes are recorded in Table IV. Luminescence was examined in acetonitrile at room temperature and in a 4:1 ethanol/methanol glass at 77 K. Luminescence was observed for $[(bpy)Ru(bpmRe(CO)_3Cl)_2]^{2+}$ and $[Ru(bpmRe(CO)_3Cl)_3]^{2+}$ at room temperature and for $(bpm)Re(CO)_3Cl$,[14] $[(bpy)_2Ru(bpmRe(CO)_3Cl)]^{2+}$, and $[(bpy)_2RuHAT(Re(CO)_3Cl)_2]^{2+}$ at 77 K.

(13) Nicholson, R. S.; Shain, I. *Anal. Chem.* **1964**, *36*, 705.

(14) This compound was reported to emit at room temperature in ref 3. Our preparative work has led us to the conclusion various luminescing intermediates can be obtained en route to $(bpm)Re(CO)_3Cl$. We plan to report the properties of one of these shortly.

Table IV. Luminescence Properties of Ruthenium(II)/Rhenium(I) Complexes[a]

complex	λ_{em},[b] nm 25 °C	77 K	τ_0,[c] ns	Φ_{em}[d]
$[(bpy)_2Ru(bpm)]^{2+}$ [e]	710		76	0.0011
$[((bpy)_2Ru)_2(bpm)]^{4+}$		769, 870[f]		
$[(bpy)_2Ru(bpmRe(CO)_3Cl]^{2+}$		630		
$[(bpy)Ru(bpmRe(CO)_3Cl)_2]^{2+}$	630	616	942	2.7×10^{-5}
$[Ru(bpmRe(CO)_3Cl)_3]^{2+}$	640	586, 650	847	2.6×10^{-5}
$[Ru(bpy)_2HAT]^{2+}$ [g]	745		105	8.0×10^{-3} [i]
$[(bpy)_2RuHAT(Re(CO)_3Cl)_2]^{2+}$	670	604, 664		
$[Ru(bpy)_3]^{2+}$ [h]	620		850	0.042

[a] In acetonitrile at 25 °C and 4:1 ethanol/methanol glass at 77 K, unless otherwise noted; λ_{ex} = 436 nm. [b] λ_{max}, nm; error ±2 nm. [c] τ_0, ±5%. [d] ±10%. [e] Propylene carbonate; from ref 8. [f] None observed in solution; solid, 769 and 870 nm: Fuchs, Y.; Lofters, S.; Dieter, T.; Shi, W.; Morgan, R.; Strekas, T. C.; Gafney, H. D.; Baker, A. D. *J. Am. Chem. Soc.* **1987**, *109*, 2691. [g] Reference 9. [h] Reference 8. [i] This work.

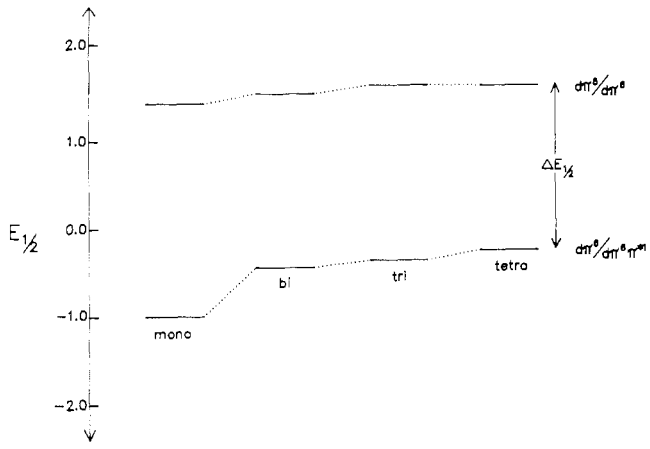

Figure 5. Comparison of redox potentials associated with the thermodynamic energy gap, $\Delta E_{1/2}$.

Emission was weak in all of these complexes. The fact that $[(bpy)Ru(bpmRe(CO)_3Cl)_2]^{2+}$ and $[Ru(bpmRe(CO)_3Cl)_3]^{2+}$ have rather long lifetimes at room temperature is of specific interest. The synthetic source materials $[Ru(bpm)_2(bpy)]^{2+}$ and $[Ru(bpm)_3]^{2+}$ have emission lifetimes at room temperature in acetonitrile of 76 and 131 ns, respectively, ruling them out as impurities in the solution.[11]

In the mixed-metal complexes, the emission appears to be ruthenium based. This is best illustrated by the long emission lifetimes of $[(bpy)Ru(bpmRe(CO)_3Cl)_2]^{2+}$ and $[Ru(bpmRe(CO)_3Cl)_3]^{2+}$. Rhenium-based emissions typically have short lifetimes on the order of 50 ns or less.

Discussion

Energy States. The physical properties of these multimetallic complexes can be interpreted in terms of weak electronic interactions of the separated metal centers. The various metal fragments can be treated initially as independent chromophores[15] and the properties adjusted for the perturbations associated with the presence of more than one metal center. The electrochemical data for $[Ru(bpy)_2(bpm)]^{2+}$ and $Re(bpm)(CO)_3Cl$ indicate that the $d\pi$ orbitals of ruthenium(II) and rhenium(I) are at approximately the same energy. Further, the reduction of the bipyrimidine ligand for each also occurs at comparable values. Thus, the energy gap expressed by $\Delta E_{1/2}$, where $\Delta E_{1/2}$ is the positive difference between the $E_{1/2}$ value for the first oxidation and the $E_{1/2}$ value for the

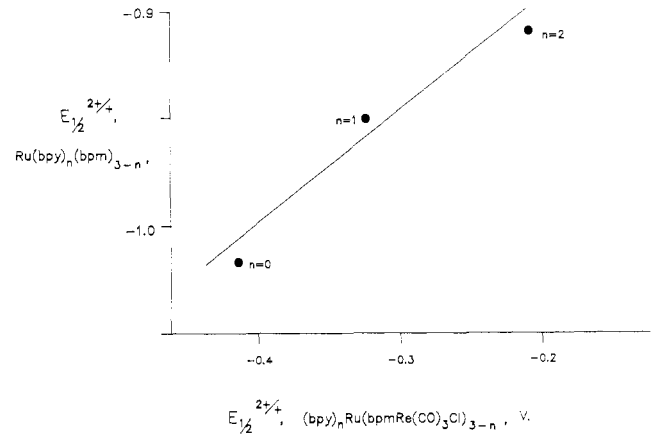

Figure 6. Correlation between the first reduction couples of the $[Ru(bpy)_n(bpm)_{3-n}]^{2+/+}$ series (vertical axis) and the $[Ru(bpy)_n(bpmRe(CO)_3Cl)_{3-n}]^{2+/+}$ series (horizontal axis), n = 0–2.

first reduction, is approximately the same for each complex. This is illustrated by the left-hand entry in Figure 5, representing the case for either $[Ru(bpy)_2(bpm)]^{2+}$ or $Re(bpm)(CO)_3Cl$. The bimetallic $(Re(CO)_3Cl)_2bpm$, $[(Ru(bpy)_2)_2bpm]^{4+}$, and $[(bpy)_2Ru(bpmRe(CO)Cl)]^{2+}$ complexes have similar redox potentials compared to their monometallic precursors. Reduction of coordinated bpm is shifted to more positive potential by 0.6 V, while the potential of the metal-centered oxidation couple is shifted positively by only about 0.1 V. The rather large shift in potential for reduction of coordinated bpm results from charge lowering of the π^* energy levels of the bridging bpm ligand due to the presence of the second metal center.[16] As shown in Figure 5, similar electrochemical changes for the trimetallic $[(bpy)Ru(bpmRe(CO)_3Cl)_2]^{2+}$ and the tetrametallic $[Ru(bpmRe(CO)_3Cl)_3]^{2+}$ are less pronounced compared to their immediate predecessor.

The trend found for the $d\pi^6/d\pi^6\pi^{*1}$ redox couple in the series tetrametallic > trimetallic > bimetallic can be understood by comparing it to the same trend found for the series $[Ru(bpm)_3]^{2+}$ > $[Ru(bpm)_2(bpy)]^{2+}$ > $[Ru(bpy)_2(bpm)]^{2+}$. This is graphically illustrated in Figure 6. The data associated with $E_{1/2}$ for the $[Ru(bpy)_n(bpm)_{3-n}]^{2+/+}$ couples are plotted on the vertical axis; those associated with $E_{1/2}$ for the $[Ru(bpy)_n(bpmRe(CO)_3Cl)_{3-n}]^{2+/+}$ couples, n = 0–2, are plotted on the horizontal axis. The slope is 0.53, the correlation coefficient is 0.96, and the intercept is −0.79 V. The important point to note from Figure 6 is that substitution of $(bpmRe(CO)_3Cl)$ for bpy in ruthenium(II) complexes results in an $E_{1/2}$ adjustment in the same direction but with approximately twice the effect noted for substitution of bpm for bpy. This most likely results from lower electron density on the bridging ligand due to back-bonding between the rhenium $d\pi$ and the bpm π^* energy levels.

The energy changes associated with spectral absorptions and emissions for Ru(II)/Re(I) complexes are illustrated in Figure 7. In this figure, the ruthenium complexes are on the left-hand side, rhenium complexes are placed on the right-hand side, and ruthenium/rhenium complexes are located in the middle. Comparisons are made between the low-energy $d\pi \rightarrow \pi^*(bpm)$ transition, the approximate position of the ^3MLCT state (when known), and the ground state. The following comments summarize the general features of Figure 7. (1) The optical transition (^1MLCT) for $Re(bpm)(CO)_3Cl$ is 0.65 eV higher in energy than the one for $[Ru(bpy)_2(bpm)]^{2+}$. (2) The ^1MLCT transitions of the homobinuclear complexes are 0.5–0.6 eV lower in energy than their monometallic precursors. (3) For the mixed-metal complexes, the ^1MLCT transition increases in energy by approximately 0.12–0.14 eV in the series $[(bpy)_2Ru(bpmRe(CO)_3Cl)]^{2+}$ < $[(bpy)Ru(bpmRe(CO)_3Cl)_2]^{2+}$ < $[Ru(bpmRe(CO)_3Cl)_3]^{2+}$. (4) Emission energies place the ^3MLCT states between 1.5 and 2.0 eV above the ground state.

(15) Brown, D., Ed. *Mixed-Valence Compounds*; Reidel: Dordrecht, The Netherlands, 1980.

(16) Callahan, R. W.; Brown, G. M.; Meyer, T. *Inorg. Chem.* **1975**, *14*, 1443.

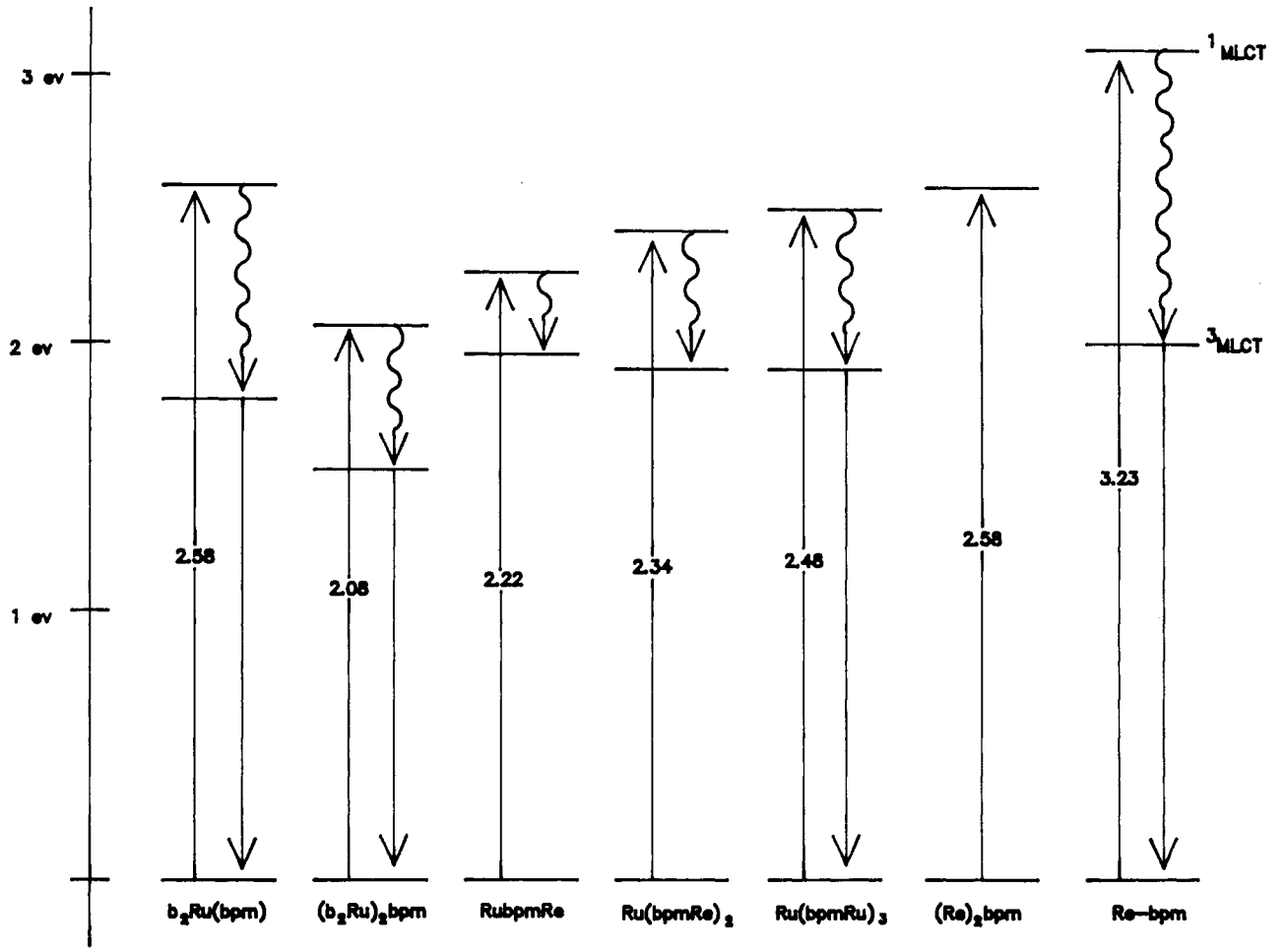

Figure 7. Comparison of the ^{1}MLCT absorption energy maxima and the ^{3}MLCT emission energy maxima for various ruthenium(II)/rhenium(I) complexes.

The energy lowering of the ^{1}MLCT transition for the binuclear complexes has been explained by charge interaction of the incoming metal center with the π^* energy levels of the bridging ligand.[17] The increase of positive charge due to the presence of the second metal center lowers the π^* energy levels of the ligand, accounting for the optical transition at lower energy. The increase in energy of the ^{1}MLCT band maxima for the mixed-metal complexes in the series bimetallic < trimetallic < tetrametallic can be understood by comparison to the optical transitions for the sequence $[Ru(bpy)_2(bpm)]^{2+}$, $[Ru(bpy)(bpm)_2]^{2+}$, and $[Ru(bpm)_3]^{2+}$. This is illustrated in Figure 8 where the ^{1}MLCT energies for the $[Ru(bpy)_n(bpm)_{3-n}]^{2+}$ series, n = 0–2, are plotted on the vertical axis and the ^{1}MLCT energies for the $[Ru(bpy)_n(bpmRe(CO)_3Cl)_{3-n}]^{2+}$ series are plotted on the horizontal axis. The correction gives a coefficient of 0.95, a slope of 0.58, and an intercept of 1.3 eV. Figure 8 illustrates that replacement of bpm by $bpmRe(CO)_3Cl$ in ruthenium complexes results in ^{1}MLCT shifts in the same direction but with approximately twice the change.

For mixed-metal complexes, there should be two ^{1}MLCT transitions related to the excited-state photophysics. One should be associated with $d\pi(Ru) \rightarrow \pi^*(bpm)$; the other should be associated with $d\pi(Re) \rightarrow \pi^*(bpm)$. The one associated with the ruthenium center is dominant. The absorption coefficients in the monometallic and homobimetallic complexes are 1 order of magnitude larger than for their rhenium(I) analogues. In addition, the transitions associated with the ruthenium center occur at lower energy. Consequently, the $d\pi(Re) \rightarrow \pi^*(bpm)$ transitions in mixed-valence complexes are masked. However, by comparison to the ^{1}MLCT transition in the monometallic and homobimetallic complexes of ruthenium and rhenium, the $d\pi(Re) \rightarrow \pi^*(bpm)$ transition in the mixed-metal systems is at higher energy than the $d\pi(Ru) \rightarrow \pi^*(bpm)$ transition.

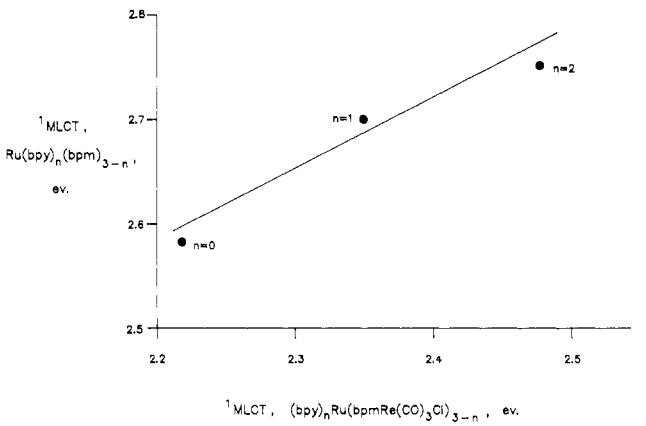

Figure 8. Correlation of the ^{1}MLCT absorption energy maxima of the $[Ru(bpy)_n(bpm)_{3-n}]^{2+}$ series (vertical axis) with the ^{1}MLCT energy maxima of the $[Ru(bpy)_n(bpmRe(CO)_3Cl)_{3-n}]^{2+}$ series, n = 0–2.

One feature of relevance to the emission properties of the ruthenium heterocycles and rhenium tricarbonyl complexes is the similar energies of their emissions. This means that the energy gap between the ^{1}MLCT and ^{3}MLCT states as shown in Figure 7 is greater for rhenium(I) tricarbonyl complexes than for ruthenium heterocycles. Thus, emission derived from the Ru(bpm) or $(bpm)Re(CO)_3$ chromophores will be at approximately the same energy, making the source of the emission difficult to assign in mixed Ru(II)/Re(I) systems.

Summary. The mixed-metal complexes of ruthenium and rhenium studied in this paper can be envisioned as having a ruthenium core with ligands $(bpmRe(CO)_3Cl)$ and HAT(Re-

(17) Sahai, R.; Morgan, L.; Rillema, D. P. *Inorg. Chem.* **1988**, *27*, 3495.

$(CO)_3Cl)_2$ attached to it. The second metal system (rhenium) perturbs the system by lowering the π^* energy levels of the bridging ligand. This lowers the energy of the ^{1}MLCT transition and the reduction potential for the $d\pi^6/d\pi^6\pi^{*1}$ couple.

Acknowledgment. We thank the Office of Energy Science of the Department of Energy for support under Grant DE-FG05-84ER-13263.

Supplementary Material Available: Table V, giving elemental analyses of some of the ruthenium(II)/rhenium(I) compounds (1 page). Ordering information is given on any current masthead page.

Contribution from the Department of Chemistry, Northern Illinois University, DeKalb, Illinois 60115

Crystal Structures and Solution Electronic Absorption and MCD Spectra for Perchlorate and Halide Salts of Binuclear Gold(I) Complexes Containing Bridging $Me_2PCH_2PMe_2$ (dmpm) or $Me_2PCH_2CH_2PMe_2$ (dmpe) Ligands

Huey-Rong C. Jaw, M. Meral Savas, Robin D. Rogers,* and W. Roy Mason*

Received August 17, 1988

Perchlorate and bromide salts of $Au_2(dmpm)_2^{2+}$ and perchlorate, chloride, bromide, and iodide salts of $Au_2(dmpe)_2^{2+}$ were crystallized and studied by X-ray diffraction. $[Au_2(dmpm)_2](ClO_4)_2$ crystallizes in the monoclinic space group $C2/m$ with a = 9.608 (5) Å, b = 13.317 (5) Å, c = 9.039 (5) Å, β = 97.50 (5)°, and D_{calcd} = 2.51 g cm^{-3} for Z = 2. The methyl group and CH_2 bridging atoms are disordered, resulting in two different chair conformations for the eight-membered cation ring. The Au···Au distance is 3.028 (2) Å. The perchlorate anions are also fractionally disordered. $[Au_2(dmpm)_2]Br_2\cdot 2H_2O$ is triclinic, $P\bar{1}$, with a = 8.005 (1) Å, b = 8.007 (3) Å, c = 10.111 (3) Å, α = 66.61 (5)°, β = 75.84 (2)°, γ = 70.70 (2)°, and D_{calcd} = 2.56 g cm^{-3} for Z = 1. The cation exists in a chair conformation with a Au···Au separation of 3.023 (1) Å. $[Au_2(dmpe)_2](ClO_4)_2\cdot H_2O$ is tetragonal, $P4_22_12$, with a = 9.486 (5) Å, c = 16.053 (3) Å, and D_{calcd} = 2.09 g cm^{-3} for Z = 2. The anion and solvent are disordered; the Au···Au distance in the cation is 2.872 (2) Å. $[Au_2(dmpe)_2]Cl_2\cdot 2H_2O$ and $[Au_2(dmpe)_2]Br_2\cdot 1.5H_2O$ are isostructural, with one anion and the water molecules disordered. The bromide analogue crystallizes with one disordered solvent site empty. Both are triclinic, $P\bar{1}$, with a = 8.661 (9) Å, b = 11.582 (6) Å, c = 13.600 (4) Å, α = 69.62 (3)°, β = 69.00 (6)°, γ = 83.87 (7)°, and D_{calcd} = 2.23 g cm^{-3} for Z = 1 (Cl) and a = 8.575 (7) Å, b = 11.841 (6) Å, c = 13.251 (9) Å, α = 71.02 (6)°, β = 71.44 (7)°, γ = 86.43 (6)°, and D_{calcd} = 2.43 g cm^{-3} for Z = 1 (Br). The Au···Au separation is 2.9265 (5) Å in the chloride and 2.9438 (5) Å in the bromide. $[Au_2(dmpe)_2]I_2\cdot CH_3CN$ is monoclinic, $P2_1/c$, with a = 10.436 (5) Å, b = 24.970 (8) Å, c = 20.383 (8) Å, β = 96.53 (4)°, and D_{calcd} = 2.49 g cm^{-3} for Z = 8. The two unique Au···Au distances average 2.974 (3) Å. Electronic absorption and magnetic circular dichroism (MCD) spectra are presented for dilute $HClO_4$ and CH_3CN solutions. The spectra of the ClO_4^- salts reveal two low-energy band systems and accompanying negative MCD B terms that are interpreted as Au_2-localized transitions $d\sigma^* \rightarrow p\sigma$. Several higher energy bands are ascribed to AuP_2-localized transitions. The spectra of the halide salts in CH_3CN do not obey Beer's law, and their concentration dependence is attributed to halide association to form $Au_2P_4X^+$ species. Association constants are determined from quantitative dependence of the spectra on cation and halide concentrations. The spectral transitions for the $Au_2P_4X^+$ species are assigned as $X^- \rightarrow Au_2^{2+}$ ligand to metal charge transfer (LMCT). The importance of Au-Au interaction in the annular complexes in the solid and in solution is discussed.

Introduction

Gold(I) forms an interesting class of binuclear complexes with certain bidentate ligands.[1-10] The structures of these complexes consist of eight-membered rings **1** in which two nearly linear two-coordinate AuX_2 units are linked together and feature a relatively short trans annular Au-Au distance. Typical values of the Au-Au distance include 2.76 (1) Å in $[Au_2(S_2CN(Pr^n)_2)_2]$,[6] 2.876 Å in $[Au_2((CH(Ph_3P))_2CO)_2]$,[10] 2.888 (3) Å in $[Au_2((Ph_2P)_2CH)_2]$,[1] 3.010 (1) Å in $[Au_2((Me_2P)_2CH_2)_2]Cl_2\cdot 2H_2O$,[4] 3.023 Å in $[Au_2((CH_2)_2PEt_2)_2]$,[9] and ~3.04 Å in $[Au_2(S_2P(OPr^i)_2)_2]$[7] (for comparison, the interatomic distance in Au metal, 2.884 Å,[11] lies within this range of Au-Au distances). The Au(I) centers in these complexes have closed-shell $5d^{10}$ electron configurations and are therefore formally nonbonded. However, at the observed distances (0.4-0.6 Å less than van der Waals contacts of 3.4 Å[12]) there is clearly significant intramolecular Au-Au interaction. The detailed nature and electronic structural consequences of this interaction are not well understood. Most of

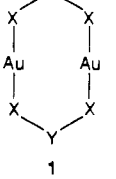

1

X = PPh_2; Y = CH,[1] CH_2,[2] NH[3]
X = PMe_2; Y = CH_2,[4] $(CH_2)_2$,[5] $(CH_2)_3$[5]
X = S; Y = CNR_2,[6] $P(OR)_2$,[7] COR[8]
X = CH_2; Y = PR_2[9]
X = $CH(PPh_3)$; Y = CO[10]

(1) Briant, C. E.; Hall, K. P. Mingos, D. M. P. *J. Organomet. Chem.* **1982**, *229*, C5. Schmidbauer, H.; Mandl, J. R.; Bassett, J.-M.; Blaschke, G.; Zimmer-Gasser, B. *Chem. Ber.* **1981**, *114*, 433.
(2) Schmidbauer, H.; Wohlleben, U. S.; Frank, A.; Huttner, G. *Chem. Ber.* **1977**, *110*, 2751.
(3) Uson, R.; Laguna, A.; Laguna, M.; Fraile, M. N.; Jones, P. G.; Sheldrick, G. M. *J. Chem. Soc., Dalton Trans.* **1986**, 291.
(4) Kozelka, J.; Oswald, H. R.; Dubler, E. *Acta Crystallogr.* **1986**, *C42*, 1007.
(5) Ludwig, W.; Meyer, W. *Helv. Chim. Acta* **1982**, *65*, 934.
(6) (a) Hesse, R.; Jennische, P. *Acta Chem. Scand.* **1972**, *26*, 3855. (b) Åkerstrom, S. *Ark. Kemi* **1959**, *14*, 387. (c) Farrell, F. J.; Spiro, T. G. *Inorg. Chem.* **1971**, *10*, 1606. (d) Miller, J. B.; Burmeister, J. L. *Synth. React. Inorg. Met.-Org. Chem.* **1985**, *15*, 223.
(7) Lawton, S. L.; Rohrbaugh, W. J.; Kokotailo, G. T. *Inorg. Chem.* **1972**, *11*, 2227.
(8) Weinstock, J.; Sutton, B. M.; Kuo, G. Y.; Walz, D. T.; DiMartino, M. J. *J. Med. Chem.* **1974**, *17*, 139.
(9) Schmidbauer, H.; Mandl, J. R.; Richter, W.; Bejenke, V.; Frank, A.; Huttner, G. *Chem. Ber.* **1977**, *110*, 2236.
(10) Vicente, J.; Chicote, M.-T.; Sauva-Llamas, I.; Jones, P. G.; Meyer-Bäse, K.; Erdbrügger, C. F. *Organometallics* **1988**, *7*, 997.
(11) Sutton, L. E., Ed. *Chemical Society Special Publication 11*; Chemical Society: London, 1958; p 53.
(12) Bondi, A. *J. Phys. Chem.* **1964**, *68*, 441.

0020-1669/89/1328-1028$01.50/0